Asociación Argentina de Mecánica Computacional

Mecánica Computacional Vol XXIX, págs. 1013-1028 (artículo completo)
Eduardo Dvorkin, Marcela Goldschmit, Mario Storti (Eds.)
Buenos Aires, Argentina, 15-18 Noviembre 2010

EQUILIBRIUM PATH ANALYSIS OF TRUSS STRUCTURES USING CONTINUATION METHODS

Fernando R. Gonçalves, Leonardo B. Lago, Jorge C. Costa, Paulo S. B. Nigro, Eduardo de M. B. Campello and Paulo de M. Pimenta

Laboratório de Mecânica Computacional da Escola Politécnica Universidade de São Paulo.

Keywords: Equilibrium path; arc length; geometrically nonlinear behavior.

Abstract. The goal of this work is to analyze and identify the post-critical behavior from trusses structures by obtaining its equilibrium path. Until the critical behavior, detection methods are sufficient for determining the critical load in the structure. However, to the entire equilibrium path, such methods have no capacity to overcome the critical point of the structure, therefore, is necessary the continuation methods, just as the arc-length. The propose models present geometrically nonlinear behavior and the structural theory adopted use exact kinematic formulation. The reach results are analyzed against benchmark problems and classical analytical results.

1 INTRODUCTION

The resolution of nonlinear systems appears with frequency in several fields of science and engineering. Especially, in structural engineering, a problem that lies in solving a nonlinear system, occurs when we want to obtain the equilibrium path, It is necessary to determine the curve that relates the displacement of a specific system options equilibrium (stable or unstable) that the structure can get to a certain level of loading.

Incremental methods as the Newton-Rapshon can reach and detect some points from them in which the structure becomes unstable, but he cannot represent all post-critical equilibrium paths. To obtain the complete curve, it is necessary to use a continuation method that allows obtaining all points to the limit of loading desired. In this work we use to obtain such path equilibrium the arc-length method described by Crisfield (1997) applied to a truss geometrically exact model developed by Pimenta (1986).

2 FORMULATION GEOMETRICALLY EXACT OF TRUSS

According to Pimenta (1986), whether the truss bars represented in its initial and deformed configuration in figure 1 below.

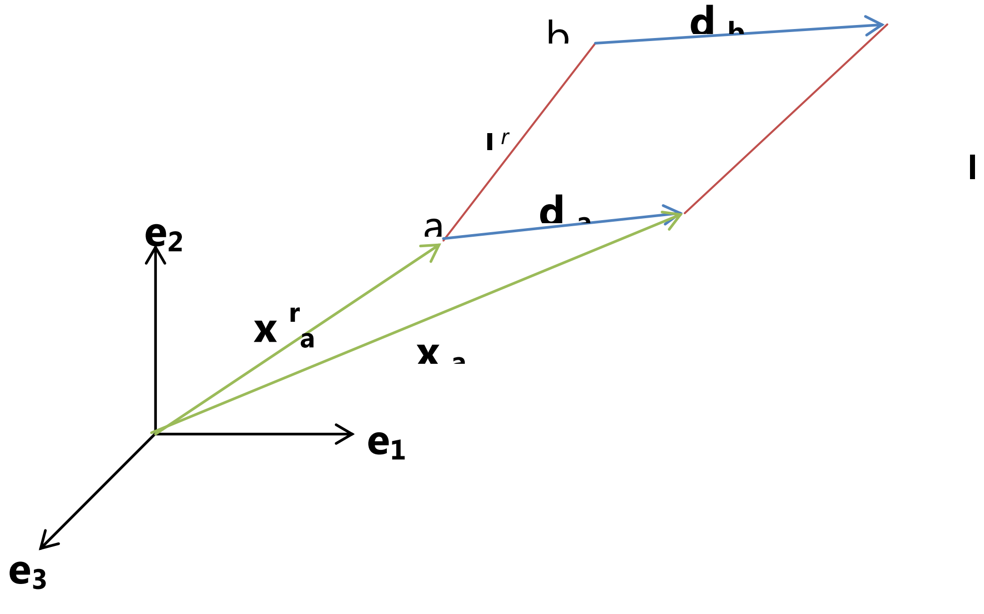

Figure 1:Kinematic configuration

The vector of nodal coordinates of element in the reference configuration $\boldsymbol{x}^r$ and the vector of nodal coordinates in the deformed configuration $\boldsymbol{x}$ are given by:

$$\boldsymbol{x}^r = \begin{bmatrix} \boldsymbol{x}_a^r \\ \boldsymbol{x}_b^r \end{bmatrix} \qquad \boldsymbol{x} = \begin{bmatrix} \boldsymbol{x}_a \\ \boldsymbol{x}_b \end{bmatrix} \tag{1}$$

Being $\boldsymbol{x}_a^r$ and $\boldsymbol{x}_b^r$ the coordinates of nodes "a" and "b" in the reference coordinates $\boldsymbol{x}_a$ e $\boldsymbol{x}_b$ the coordinates of nodes "a" and "b" in the deformed configuration. The vector $\boldsymbol{\lambda}$ that associates the direction of the bar with direction appointed of "a" to "b" may be represented by:

$$\boldsymbol{\lambda} = \boldsymbol{\Psi}\boldsymbol{x}_e = \begin{bmatrix} -\boldsymbol{I}_3 & \boldsymbol{I}_3 \end{bmatrix}\boldsymbol{x}_e$$

$$\boldsymbol{\Psi} = \begin{bmatrix} -\boldsymbol{I}_3 & \boldsymbol{I}_3 \end{bmatrix} \tag{2}$$

The matrix $\boldsymbol{I}_3$ is the identity matrix of order 3. The nodal displacements can be represented by:

$$\boldsymbol{d} = \begin{bmatrix} \boldsymbol{d}_a \\ \boldsymbol{d}_b \end{bmatrix} = \begin{bmatrix} \boldsymbol{x}_a - \boldsymbol{x}_a^r \\ \boldsymbol{x}_b - \boldsymbol{x}_b^r \end{bmatrix} \tag{3}$$

The vector modulus $\boldsymbol{\lambda}$ is 1, then:

$$\lambda^2 = \boldsymbol{\lambda}^T\boldsymbol{\lambda} = \boldsymbol{x}_e^T\boldsymbol{\Psi}^{\mathbf{T}}\boldsymbol{\Psi}\boldsymbol{x}_e \tag{4}$$

The stretching is given by:

$$\Lambda = \sqrt{\boldsymbol{\lambda}^T\boldsymbol{\lambda}} / \lambda^r \tag{5}$$

The virtual increase of bar length is given by stretching variation:

$$\delta\lambda = \lambda^{-1}\boldsymbol{x}^T\boldsymbol{\Psi}^T\boldsymbol{\Psi}\delta\boldsymbol{x}_e = \lambda^{-1}\boldsymbol{\lambda}^T\boldsymbol{\Psi}\delta\boldsymbol{x}_e \tag{6}$$

The virtual work of internal strength of a truss is given bellow jointly with the internal forces vector from the truss $\boldsymbol{r}_e$:

$$\delta W_I = V^r \boldsymbol{\varepsilon}_m \Lambda^{2m} l^{-2} \mathbf{l}^T \boldsymbol{\Psi} \delta \boldsymbol{x}_e = \boldsymbol{r}_e^T \delta \boldsymbol{x}_e$$
$$\boldsymbol{r}_e = V^r \boldsymbol{\varepsilon}_m \Lambda^{2m} l^{-2} \boldsymbol{\Psi}^T \mathbf{l} \tag{7}$$

V^r is the truss volume in reference configuration, being that $V/V^r \approx 1$. Where the family of strain measure is defined through:

$$\boldsymbol{\varepsilon}_m = \begin{cases} \left(\Lambda^{2m} - 1\right)/2m, & m \neq 0 \\ \ln \Lambda, & m = 0 \end{cases} \tag{8}$$

To this work, the m value is considered 1, which represents Green's strain. The total virtual work from internal forces of structure is given by:

$$\delta W_I = \sum_{e=1}^{Nel} \boldsymbol{r}_e^T \delta \boldsymbol{x}_e = \sum_{e=1}^{Nel} \boldsymbol{r}_e^T A_e \delta \boldsymbol{x} \tag{9}$$

Where A_e is a filled matrix with zeros and ones, which lists the degree of freedom of an element with degree of freedom of structure and Nel is the total number of bars from structure. The virtual work of external forces is provided by:

$$\delta W_E = \boldsymbol{f}_{ext}^T \delta \boldsymbol{x} \tag{10}$$

Where $\boldsymbol{f}_{ext}$ is the external forces vector applied on nodes of structure. For virtual work theorem, can be match (9) and (10), coming in:

$$\boldsymbol{f}_{ext} - \boldsymbol{r} = 0 \tag{11}$$

$$\boldsymbol{r} = \sum_{e=1}^{Nel} \boldsymbol{A}_e^T \boldsymbol{r}_e \tag{12}$$

Deriving by the time (11) can be obtained the equations which describe the incremental balance from structure:

$$\dot{\boldsymbol{f}}_{ext} - \dot{\boldsymbol{r}} = 0 \tag{13}$$

$\dot{\boldsymbol{f}}_{ext}$ is the boundary condition, since (12) deriving coming to $\dot{\boldsymbol{r}}$:

$$\dot{\boldsymbol{r}} = \sum_{e=1}^{Nel} \boldsymbol{A}_e^T \dot{\boldsymbol{r}}_e \tag{14}$$

Being that $\dot{\boldsymbol{r}}_e$ is obtained by derivation (7) and with mathematical coming to:

$$\begin{aligned}\dot{\boldsymbol{r}}_e &= V^r \Lambda^{2m} \left[(2m-2)\lambda^{-4} \boldsymbol{\varepsilon}_{\boldsymbol{m}} \boldsymbol{\Psi}^T \boldsymbol{\xi}\boldsymbol{\xi}^T \boldsymbol{\Psi} + \Lambda^{2m}\lambda^{-4} \boldsymbol{D}_{\boldsymbol{m}} \boldsymbol{\Psi}^T \boldsymbol{\lambda\lambda}^T \boldsymbol{\Psi} \lambda^{-2} \boldsymbol{\varepsilon}_{\boldsymbol{m}} \boldsymbol{\Psi}^T \boldsymbol{\Psi} \right] \dot{\boldsymbol{\xi}}_e \\ \dot{\boldsymbol{r}}_e &= \left(\boldsymbol{K}_G + \boldsymbol{K}_M\right) \dot{\boldsymbol{\xi}}_e\end{aligned} \tag{15}$$

$$\begin{aligned}\boldsymbol{K}_G &= V^r \Lambda^{2m} \left[(2m-2)\lambda^{-4} \boldsymbol{\varepsilon}_{\boldsymbol{m}} \boldsymbol{\Psi}^T \boldsymbol{\xi}\boldsymbol{\xi}^T \boldsymbol{\Psi} \lambda^{-2} \boldsymbol{\varepsilon}_{\boldsymbol{m}} \boldsymbol{\Psi}^T \boldsymbol{\Psi} \right] \\ \boldsymbol{K}_M &= V^r \Lambda^{4m} \lambda^{-4} \boldsymbol{D}_{\boldsymbol{m}} \boldsymbol{\Psi}^T \boldsymbol{\lambda\lambda}^T \boldsymbol{\Psi}\end{aligned} \tag{16}$$

$\boldsymbol{K}_G$ is the geometrically stiffness matrix and $\boldsymbol{K}_M$ is the constitutive stiffness matrix of element and $\boldsymbol{D}_{\boldsymbol{m}}$ is the modulus of elasticity defined by:

$$\boldsymbol{D}_m = \frac{\partial \boldsymbol{\sigma}_{\boldsymbol{m}}}{\partial \boldsymbol{\varepsilon}_{\boldsymbol{m}}} \tag{17}$$

The $\boldsymbol{\sigma}_{\boldsymbol{m}}$ is the conjugated stress related to $\boldsymbol{\varepsilon}_{\boldsymbol{m}}$.

3 CRISFIELD ARC-LENGTH METHOD

The arc-length method, generally speaking, is a solution strategy in which the path through a converged solution, at any step, follows a direction orthogonal to the tangent of the solution curve. In this procedure, both the load vector and the displacement vary. The method is presented in the in two forms. First the arc-length method is introduced in its general formulation; this is followed by the presentation of the method in a discrete formulation, as implemented in computer programs. The algorithm bellow is based in the work of Ritto-Corrêa and Camotin (2007) and Tiago (2007).

3.1 The linearized equilibrium equation

The equilibrium equation can be written:

$$\boldsymbol{g}(\boldsymbol{d},\lambda) = \boldsymbol{r}(\boldsymbol{d}) - \lambda \boldsymbol{f_{ext}} = \boldsymbol{0} \tag{18}$$

Being λ the load factor. With an iterative strategy is possible to get a collection of points describing the path equilibrium. The Newton-Raphson method can be formulated using the Taylor's series expansion in the equilibrium equation around A point,

$$\boldsymbol{g}_B = \boldsymbol{g}_A + \boldsymbol{K}_A\Delta\boldsymbol{d} - \Delta\lambda \boldsymbol{f_{ext}} + \ldots = \boldsymbol{0} \tag{19}$$

where $\boldsymbol{g}_A$ and $\boldsymbol{g}_B$ are the out-of-balance nodal forces evaluated at A and B point. The tangent matrix $\boldsymbol{K}$ and the tangent load vector $\boldsymbol{q}$ can be written,

$$\begin{aligned}\boldsymbol{K(d)} &= \frac{\partial \boldsymbol{g(d)}}{\partial \boldsymbol{d}} \\ \boldsymbol{q(d)} &= \frac{\partial \boldsymbol{f}_{ext}\boldsymbol{(d,\lambda)}}{\partial \lambda} = -\frac{\partial \boldsymbol{g(d,\lambda)}}{\partial \lambda}\end{aligned} \tag{20}$$

The solution of equation (19) can be represented by:

$$\boldsymbol{\Delta d} = \Delta\chi\boldsymbol{\delta g} + \Delta\lambda\boldsymbol{\delta q} \tag{21}$$

Being $\Delta\chi$ a non-dimensional quantity $(0 < \Delta\chi \leq 1)$. So due to (21), results:

$$\begin{aligned}\boldsymbol{\delta g} &= -\boldsymbol{K_A}^{-1}\boldsymbol{g_A} \quad \text{or} \quad \boldsymbol{K_A\delta g} = -\boldsymbol{g_A} \\ \boldsymbol{\delta q} &= \boldsymbol{K_A}^{-1}\boldsymbol{q_A} \quad \text{or} \quad \boldsymbol{K_A\delta q} = \boldsymbol{q_A}\ .\end{aligned} \tag{22}$$

Defining the vector $\boldsymbol{t}$ tangent to the path equilibrium, can be written, around B point,

$$\boldsymbol{t_B} = \begin{bmatrix}\boldsymbol{d_B} \\ \lambda_B\end{bmatrix} = \begin{bmatrix}\boldsymbol{d_A} \\ \lambda_A\end{bmatrix} + \begin{bmatrix}\boldsymbol{\Delta d} \\ \Delta\lambda\end{bmatrix} = \begin{bmatrix}\boldsymbol{d_A} \\ \lambda_A\end{bmatrix} + \Delta\chi\begin{bmatrix}\boldsymbol{\delta g} \\ 0\end{bmatrix} + \Delta\lambda\begin{bmatrix}\boldsymbol{\delta q} \\ 1\end{bmatrix} \tag{23}$$

or simply,

$$\boldsymbol{t_B} = \boldsymbol{t_A} + \Delta\chi\boldsymbol{tg} + \Delta\lambda\boldsymbol{tq} \tag{24}$$

The predictor-corrector approach consists in two steps. First, in the predictor step calculates an approximation of the desired quantity, then in the corrector step do an iterative refinement.

Predictor: from a point of equilibrium and previously calculated by applying a slight variation in the value $\Delta\lambda$ predicts the new value of the displacement, $\boldsymbol{d}_B = \boldsymbol{d}_O + \Delta\lambda\boldsymbol{\delta q}$.

Corrector: from a non-equilibrium point *A,* corrects displacement by, $\boldsymbol{d}_B = \boldsymbol{d}_A + Dc\boldsymbol{dg} + Dl\,\boldsymbol{dq}$, keeping the load parameter unchanged, or updating by $l_B = l_A + Dl$, until convergence.

3.2 The constrain equation

Setting the following dot product by

$$\boldsymbol{t_A} \circ \boldsymbol{t_B} = \boldsymbol{d_A}^t \boldsymbol{d_B} + y^2 l_A l_B \tag{25}$$

being y^2 a scaling factor that makes the product dimensionally consistent. The arc-length measured DS is the norm of vector $(\boldsymbol{t} - \boldsymbol{t_O})$, then the constrain equation can be written:

$$DS^2 = \left\| \boldsymbol{t} - \boldsymbol{t_O} \right\| = (\boldsymbol{d} - \boldsymbol{d_O})^t (\boldsymbol{d} - \boldsymbol{d_O}) + y^2 (l - l_O) \tag{26}$$

3.3 Crisfield's method

Assuming that *A* and *B* two successive points obtained in the course of the iterative process and considering equation (24),

$$\boldsymbol{t_B} - \boldsymbol{t_O} = \boldsymbol{t_A} - \boldsymbol{t_O} + Dc\boldsymbol{tg} + Dl\,\boldsymbol{tq} \tag{27}$$

And using the dot product defining in (25),

$$DS^2 = (\boldsymbol{t_A} - \boldsymbol{t_O} + Dc\boldsymbol{tg} + Dl\,\boldsymbol{tq}) \circ (\boldsymbol{t_A} - \boldsymbol{t_O} + Dc\boldsymbol{tg} + Dl\,\boldsymbol{tq}) \tag{28}$$

which results:

$$\begin{aligned} & a_1 Dl^2 + a_2 Dl + a_3 = 0 \\ & a_1 = \boldsymbol{dq}^t \boldsymbol{dq} + y^2 \\ & a_2 = \boldsymbol{dq}^t (\boldsymbol{Dd_A} + Dc\boldsymbol{dg}) + 2y^2 (l_A - l) \\ & a_3 = (\boldsymbol{Dd_A} + Dc\boldsymbol{dg})^t (\boldsymbol{Dd_A} + Dc\boldsymbol{dg}) + y^2 (l_A - l)^2 - D\bar{S}^2 \end{aligned} \tag{29}$$

Where $D\bar{S}^2$ is prescript arc-length. For the predictor using: $(\boldsymbol{d}_A - \boldsymbol{d_O}) = \boldsymbol{0}$, $(l_A - l_{\boldsymbol{O}}) = 0$, $\boldsymbol{dg} = \boldsymbol{0}$, then (29) becomes:

$$Dl_P = \frac{c_q DS}{\sqrt{\boldsymbol{dq}^t \boldsymbol{dq} + y^2}} \tag{30}$$

where the signal is positive in first load step, afterward based in the previous increment. Thus, at the end of an increment, $\Delta\lambda_P$ has a sign of

$$\chi_\theta = \begin{cases} 1 & \text{if } \ \boldsymbol{t\theta} \circ (\boldsymbol{t} - \boldsymbol{t}_0) \geq 0 \\ -1 & \text{otherwise} \end{cases} \tag{31}$$

to correct the forward direction of the equilibrium path. For de subsequent iterations $\Delta\lambda_C$ is a roots of quadratic equation (29), such that,

$$\Delta\lambda_C = \begin{cases} \Delta\lambda_1 & \text{if } \ t\Delta\lambda_1 > t\Delta\lambda_2 \\ \Delta\lambda_2 & \text{otherwise} \end{cases} \tag{32}$$

While, $a_2^2 - 4a_1a_3 > 0$, the roots stay in real values. When this condition is not met, the usual practice consists of cutting the step length down to half and resuming the iterative procedure with a new prediction, followed by new correction.

3.4 The flow chart Crisfield's algorithm – Tiago (2007)

Input data:

i - number of steps
i_{MAX} - maximum number of steps
j - number of iteration
j_{MAX} - maximum number of iteration
λ_{MAX} - maximum load factor
λ_{MIN} - minimum load factor
$\Delta\lambda$ - variation load factor
I_{DES} - desired number of iteration
$OOBtol$ - out-of-balance tolerance
$dtol$ - displacement tolerance
tol_{MAX} - maximum out-of-balance

Variables data:

l - current load factor

Dl_{inc} - variational incremental load factor

Dl_{old} - variational old load factor

$\boldsymbol{d}$ - current displacement

$\boldsymbol{d_{inc}}$ - incremental displacement

$\boldsymbol{d_{iter}}$ - iterative displacement

$\boldsymbol{d_{oldinc}}$ - old incremental displacement

$\boldsymbol{d_{fextiter}}$ - displacement due to external forces

$\boldsymbol{d_{riter}}$ - displacement due to internal forces

$\boldsymbol{f_{ext}}$ - external forces

$\boldsymbol{r}$ - internal forces

$\boldsymbol{K}$ - global stiffness

j_p - save number of iterations performance

$OOB_{\boldsymbol{conv}}$ - out-of-balance convergence test

$d_{\boldsymbol{conv}}$ - displacement convergence test

$Abs_{\boldsymbol{fext}}$ - external force absolute value

Algorithm functions:

$\hat{\boldsymbol{K}}$ - calculate global stiffness update

$\hat{\boldsymbol{r}}$ - calculate force update

$D\hat{l}_C$ - calculate and chose the root acording to (30)

$D\hat{l}_P$ - calculate and correct the sign acording to (32)

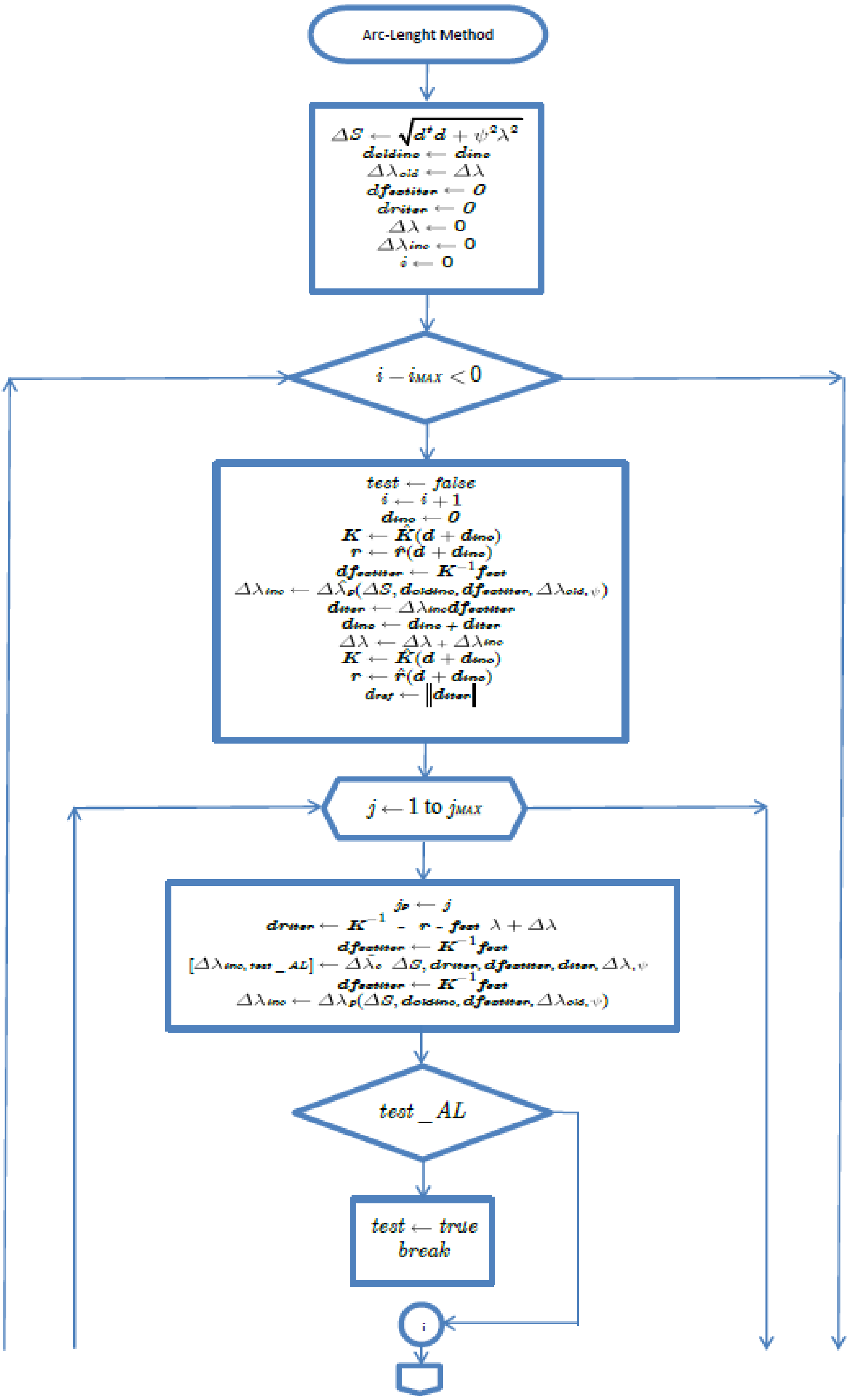

Figure 2 – Flow chart.

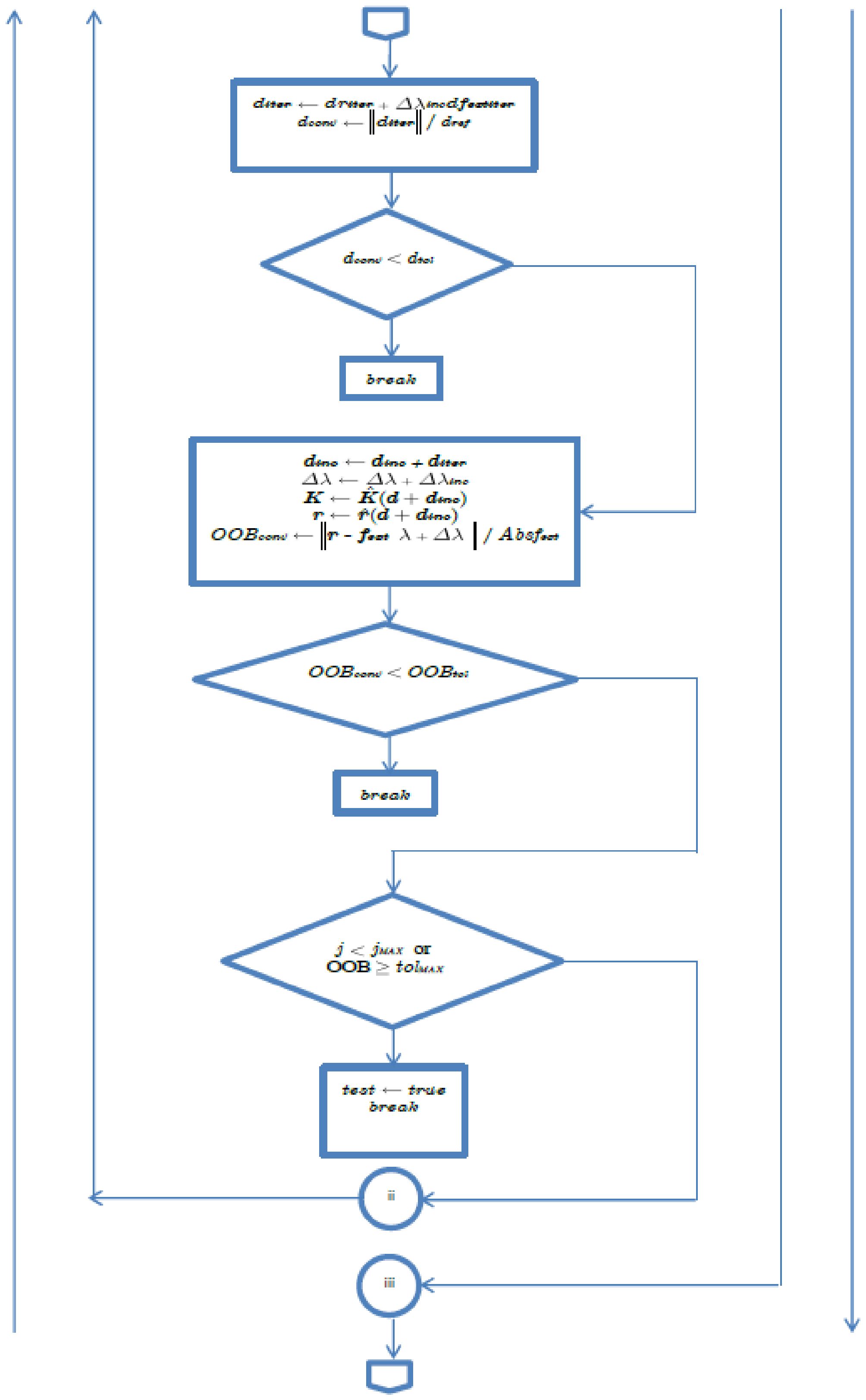

Figure 3: Flow chart continuation.

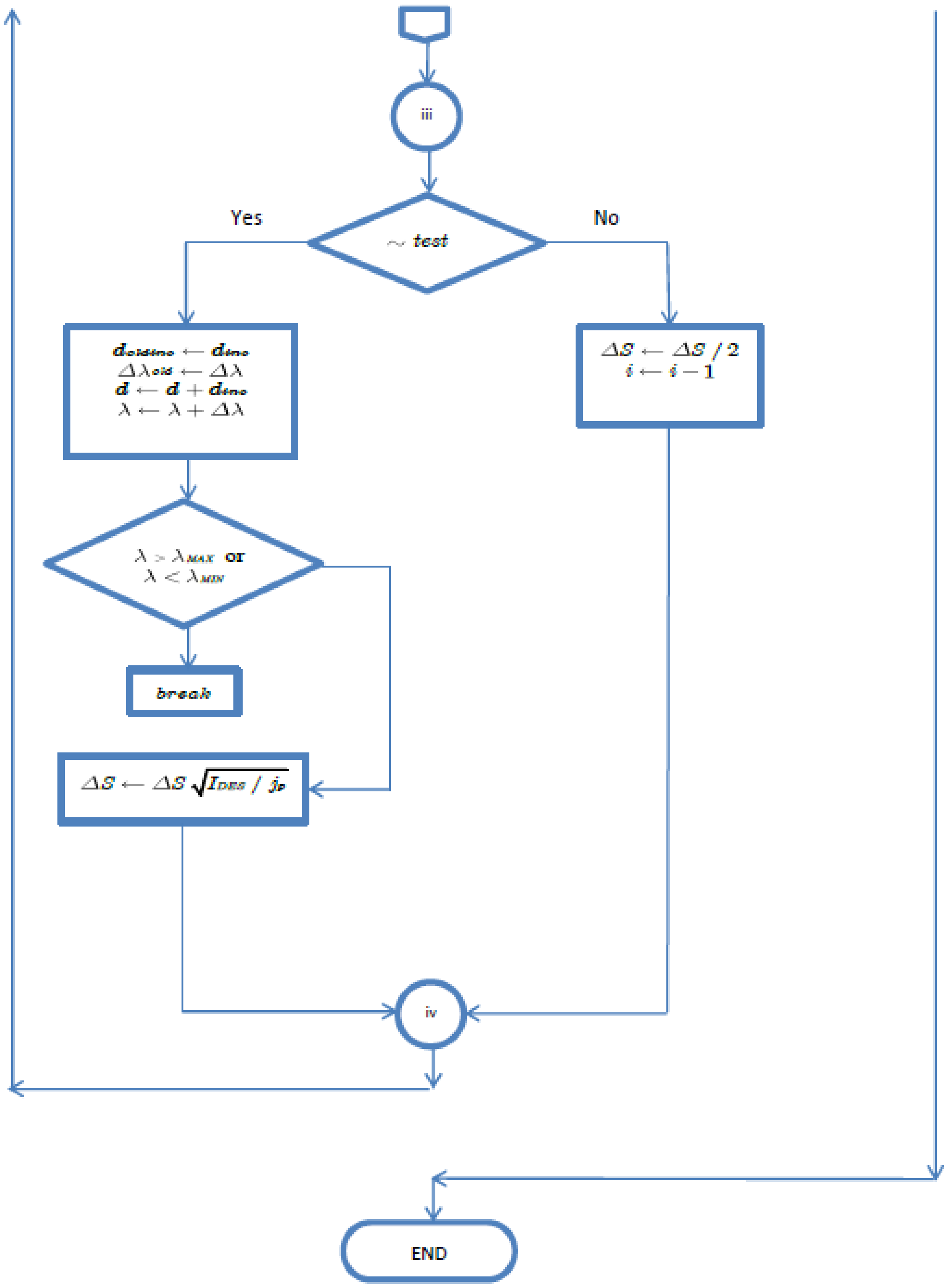

Figure 4: Flow chart continuation.

4 Examples

First example: Fafard and Massicotte (1991)

EA(1)=1000 and EA(2)=500

Bar1: (0.000, 0.000)-(0.965, 3.000)

Bar2: (0.965, 3.000)- (1.930, 0.000)

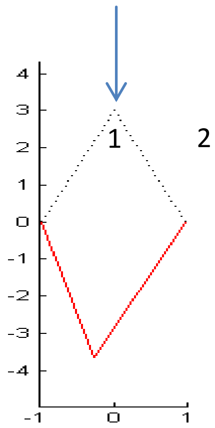

Figure 5: Initial and current truss configuration.

The graphics below show themselves consistent with the results obtained by Fafard (1991). The load factor, in our models represents the own load because they use such as loading a unit load, which will be varied by the load factor.

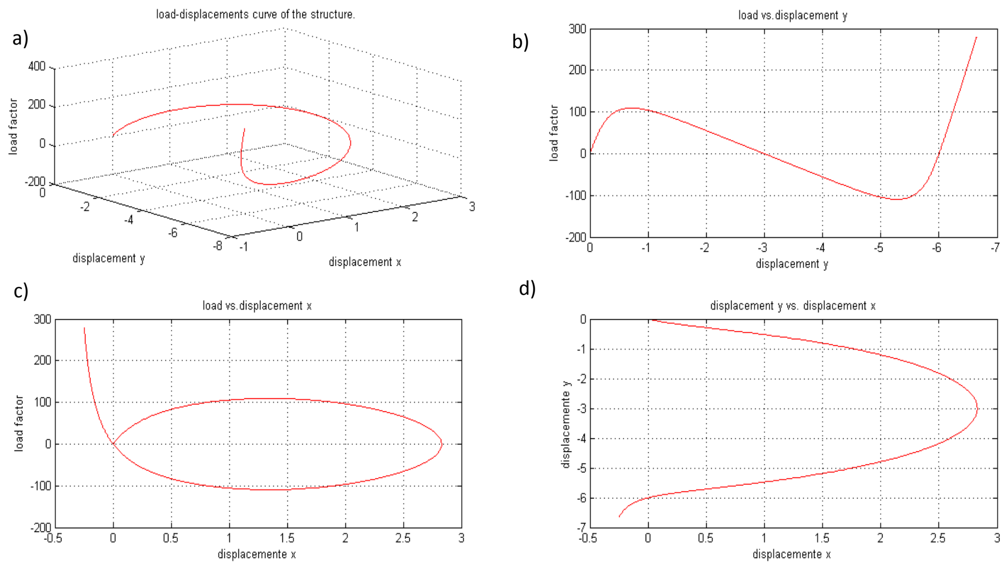

Figure 6: a) path equilibrium 3D; b) path equilibrium to y direction; c) path equilibrium to x direction; d) trajectory of load application point.

Second example: Arch Truss – Hrinda (2006)

Arch truss with 101 elements and 126 dof, its geometry can be found in Hrinda (2006) or in Crisfield (1997), EA=$1,00\times10^{7}$

a)

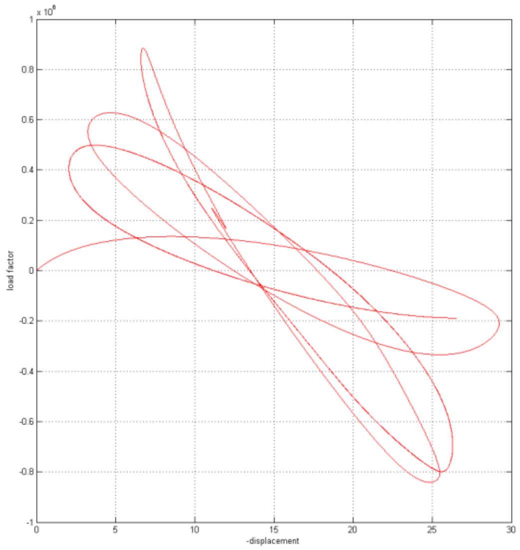

b)

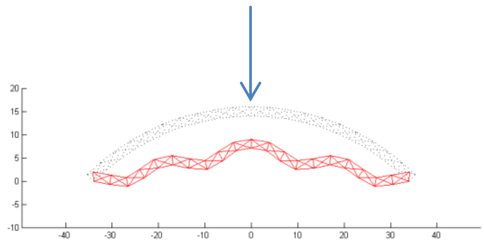

Figure 7: a) path equilibrium; b) Initial and current truss configuration.

The curve confirms the results obtained by Hrinda (2006). The curve obtained can achieve results beyond those obtained in the article that was used as a comparison.

Third Example: Sixteen-Member Shallow Truss – Hrinda (2006)

3D Structure with 16 elements and 15 dof, its geometry can be found in [3], EA=$1,00\times10^{7}$.

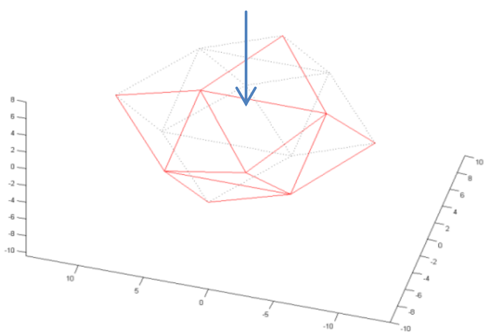

Figure 8: Initial and current truss configuration.

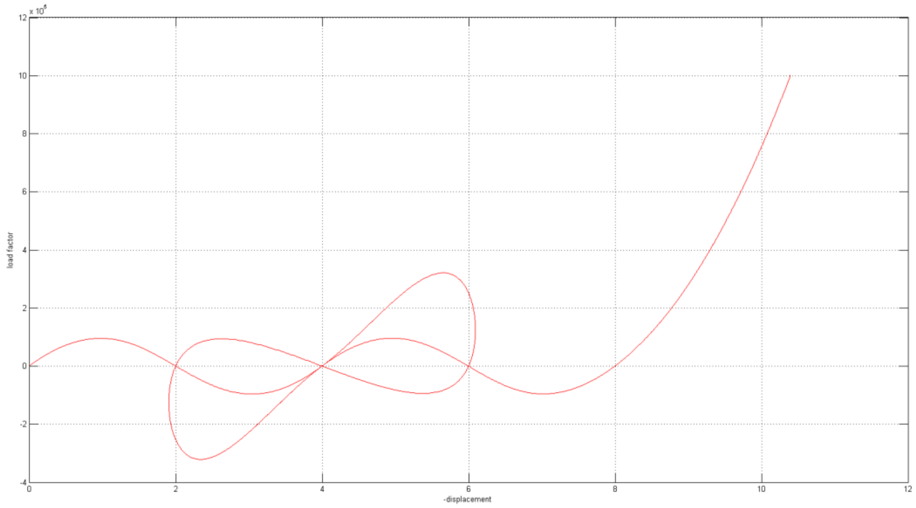

Figure 9: path equilibrium.

Again, the curve which is in agreement obtained by Hrinda (2006)

5 CONCLUSION

Aiming to validate the computational implementation based on the formulation presented in section 2 and to evaluate its effectiveness, we analyzed three examples with numerical results already established in the literature. From these examples, it can be observed that the results from formulation of nonlinear analysis of spatial trusses geometrically exact in Pimenta (1986) are consistent with other authors.

The strategy of non-linear solution becomes more significant as the equilibrium path becomes more nonlinear. The values of the load-displacement curve provided by the literature are reproduced only with the use of arc-length method, in this case the version implemented by Crisfield (1997). This method uses not only load control, displacement control but also for overcoming the limit trajectory points of equilibrium, making possible to obtain the complete curve.

Arc-length adopted allowed the observation of behavior of snap-through and snap-back that appeared in the structures shown in the examples. It cannot be affirmed that this method always works, however, it possible reach the equilibrium trajectory of several 2D and 3D structures, with symmetries or not, with nonlinearity from geometry or the material.

6 REFERENCES

Crisfield, M.A. Non-linear Finite Element Analysis of Solids and Structures**.** Vol. 2. WILEY 1997.

Fafard, M. and Massicotte, B. Geometrical Interpretation of the Arc-Length Method. *Computers and Structures*. Vol. 46, No. 4, 603-615, 1993.

Hrinda, G.A. Snap Through Instability Patterns in Truss Structures. NASA Langley Research Center, Hampton, Virginia, USA. *American Institute of Aeronautics and Astronautics*, 2006.

Pimenta, P.M. Análise não linear de treliças espaciais. *Boletim técnico da Escola Politécnica da Universidade de São Paulo*. São Paulo. Brazil, 1986.

Ritto-Corrêa, M. and Camotim, D. On the arc-length and other quadratic control methods: Established, less known and new implementation procedures. *Computer and Structures* 86 (2008) 1353-1368, 2007.

Tiago, T.F. Carlos Manuel Tiago. Meshless methods: Extending the linear formulation and its generalization to geometrically exact structural analysis. *Doctored thesis. Instituto Superior Técnico da Universidade Técnica de Lisboa*, 2007.